

Design of Active/Passive Hybrid Compliance in the Frequency Domain

– Shaping Dynamic Compliance of Humanoid Shoulder Mechanism –

Masafumi OKADA^{*1}, Yoshihiko NAKAMURA^{*1*2} and Shin-ichiro HOSHINO^{*1}

^{*1}Dept. of Mechano-Informatics, University of Tokyo
7-3-1 Hongo Bunkyo-ku Tokyo, 113 Japan

^{*2}CREST Program, Japan Science and Technology Corporation
e-mail : okada@ynl.t.u-tokyo.ac.jp

Abstract

Design and control of mechanical compliance would be one of the most important technical foci in making humanoid robots really interactive with the humans. For task execution and safety insurance the issue must be discussed and offers useful and realistic solutions. In this paper, we propose a theoretical design principle of mechanical compliance. Passive compliance implies a mechanically embedded compliance in drive systems and is reliable but not-tunable in nature, while active compliance is a controlled compliance and, therefore, widely tunable, but less reliable specially in high frequency domain. The basic idea of this paper is to use active compliance in the lower frequency domain and to rely on passive compliance in the higher frequency. H_∞ control theory based on systems identification allows a systematic method to design the hybrid compliance in frequency domain. The proposed design is applied to the shoulder mechanism of a humanoid torso robot. Its implementation and experiments are to be shown with successful results.

1 Introduction

Humanoid robots which share the space and environments with human, should have compliance. There are two approaches to realize the robot compliance. One is active compliance based on control theories on which many researches have been reported [1]~[6], the other is passive compliance adopting the mechanical elasticity. The former is known to have a limited performance in high frequency due to the small resolution of sensors, the finite sampling time and the limited actuator power, and the noise in signals. The latter is effective in all frequency while it is difficult to design the parameters, and impossible to change them adap-

tively.

This paper proposes the hybrid design of compliance in the frequency domain from the following two standpoints. (1) Frequency dependent design and (2) Hybrid implementation of active and passive compliance. Compliance in high frequency is concerned to ensure safety requirements, while that in low frequency must be carefully tuned to satisfy stationary requirements such as positioning accuracy. Thus, the requirements on compliance would be better fulfilled if it is designed in frequency domain. The first standpoint represents this consideration. The second standpoint, on the other hand, is from the robustness consideration. Implementation of compliance in frequency domain would be significantly difficult in high frequency. To overcome this, it is proposed in this paper to use both active and passive compliance. The H_∞ control theory [8] plays an important roll, in sharing compliance in frequency domain between active compliance and passive one.

We designed and fabricated the ‘cybernetic shoulder’ [7], a three degrees-of-freedom shoulder mechanism for humanoids. This mechanism has advantages such as (1) large mobile area, (2) singularity-free, (3) human-like motion of the center of rotation and (4) ease to introduce passive compliance. The active/passive hybrid implementation of compliance is applied to and experimentally verified with the torso robot with the cybernetic shoulder.

2 Passive compliance

2.1 The cybernetic shoulder and its compliance

Figure 1 shows the model of the cybernetic shoulder, where β and δ are two degrees-of-freedom gim-

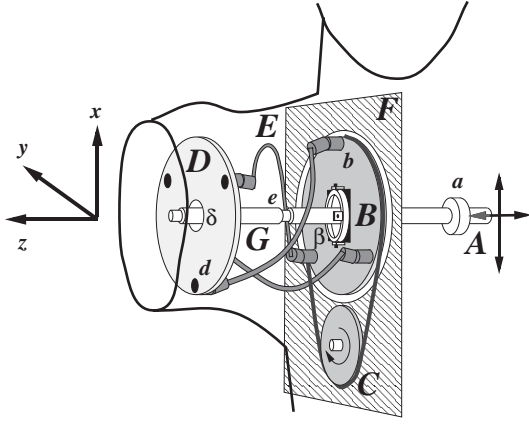


Figure 1: Cybernetic shoulder

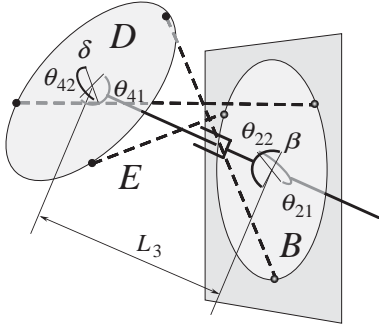


Figure 2: Definition of rotations

bal mechanisms, d is a three degrees-of-freedom ball joint, b is a two degrees-of-freedom universal joint, a is a four degrees-of-freedom joint of spherical and prismatic motion, and e is a prismatic joint. Moving point A within vertical plane alters the pointing direction of the main shaft G , which determines, along with the constraints due to the free curved links E between points b and d , the direction of the normal vector of D . The rotation about the normal of D is mainly determined by the rotation of C through B and G . Note that the rotation of C is coupled with the pointing direction of D when B and D are not parallel.

By the definition of θ_{21} , θ_{22} , θ_{41} and θ_{42} which are rotation angle of gimbal mechanisms on β and δ shown in figure 2, constraints given by links E are written in the following equations.

$$\left| (I - R_{\theta_{21}}^y R_{\theta_{22}}^x L_{L_3}^z R_{\theta_{41}}^x R_{\theta_{42}}^y R_{\pi}^z) R_{\frac{\pi}{2}(i-1)}^z r \right| = \ell_i \quad (i = 1, 2, 3) \quad (1)$$

$$r := [|b| \ 0 \ 0 \ 1]^T \quad (2)$$

Where R_{θ}^{ξ} implies the rotation of θ about ξ axis, and

L_{ℓ}^{ξ} implies the translation of ℓ along ξ axes. ℓ_i is the length of link E , $|b|$ is the diameter of B and D .

Consider that links E has elasticity. From equation (1), we can obtain

$$\begin{bmatrix} \Delta\theta_{41} \\ \Delta\theta_{42} \\ \Delta L_3 \end{bmatrix} = J_s(\theta_{21}, \theta_{22}) \begin{bmatrix} \Delta\ell_1 \\ \Delta\ell_2 \\ \Delta\ell_3 \end{bmatrix} \quad (3)$$

Using this jacobian J_s and defining spring constants of each links E as k_1 , k_2 and k_3 , the compliance matrix C_s for rotation about θ_{41} , θ_{42} and translation along L_3 is represented as

$$C_s = J_s \begin{bmatrix} k_1 & 0 & 0 \\ 0 & k_2 & 0 \\ 0 & 0 & k_3 \end{bmatrix}^{-1} J_s^T \quad (4)$$

We can calculate and design compliance of the end of the shoulder using C_s .

2.2 Design of the elastic link

We design three types of elastic or viscous link as follows.

1. Rigid link (square measure is $7 \times 10 [\text{mm}^2]$, made from duralumin, in left hand side of figure 3)
2. Elastic link ($\phi 5 [\text{mm}]$ carbon fiber, in center of figure 3)
3. Elastic and viscous link (link (2) + damper, in right hand side of figure 3)

We use ‘Temper Foam’ as a vibration absorber on link 3. This material has high viscosity in high frequency and has low viscosity in low frequency. Because the length of these links (shown by the arrow in figure 3) define the constraint of the position and orientation of the shoulder mechanism as in equation (1), we measure the spring constants and coefficients of viscosity of these links. The values of these parameters are shown in Table 1. Type 2 is more elastic than type 1, and type 3 is more viscous than type 1 and 2.

Table 1: Spring constant and coefficient of viscosity

Type	Spring constant [N/m]	Coefficient of viscosity [kg/s]
1	1.609×10^3	0.625
2	5.963×10^2	0.45
3	5.963×10^2	1.05

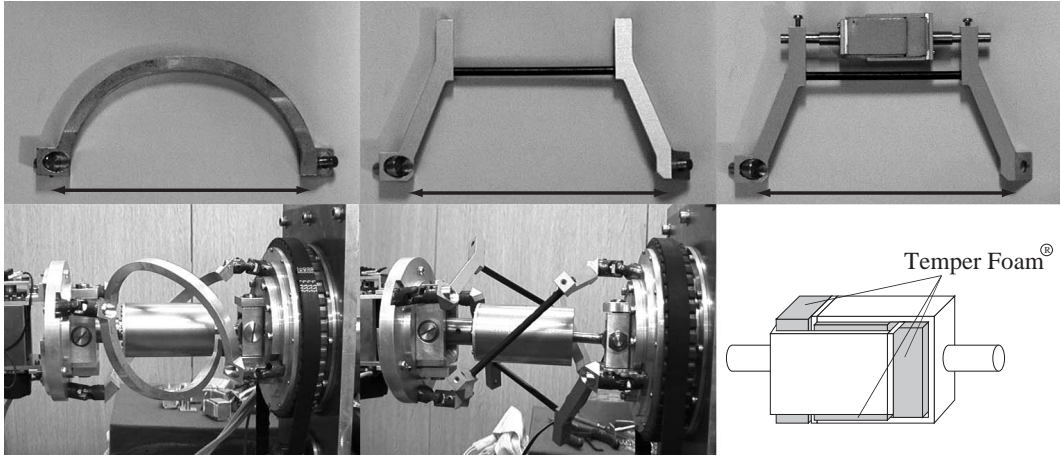


Figure 3: The cybernetic shoulder with the rigid or elastic link

2.3 Compliance of the torso robot

We have developed a torso robot using the cybernetic shoulder with above three types of links shown in figure 4, and measured the compliance of the end of the arm, where only compliance on the vertical position was measured in the specific position of the arm. The experimental configuration is shown in figure 5. By detaching 1 kg weight being hung from the end of the arm, the external force are given, and the position of the end of the arm is measured by a laser position sensor. The position of the end of the arm is

$$\begin{bmatrix} e x_0 & e y_0 & e z_0 \end{bmatrix} = \begin{bmatrix} 400 & -300 & 270 \end{bmatrix} [\text{mm}] \quad (5)$$

in the absolute coordinate. Figure 6 and 7 show the experimental results and the spectrum analysis of the oscillations. The time sequence signal is filtered by the window function $W_{\text{window}}(s)$

$$W_{\text{window}}(s) = \frac{100^4}{(s + 100)^4} \quad (6)$$

for noise attenuation. We can realize the elastic torso robot by using the carbon fiber link and the viscous torso robot using the damper.

3 Hybrid compliance in the frequency domain

We define the transfer function from the outer force f to the strain of the end of arm Δ_y as G_{yf} when f acts on the end of arm, whose gain characteristic represents the dynamic compliance of P .

The general mechanical dynamic compliance is represented by the dashed line in figure 8. It has a mechanical resonance mode. For humanoid robots which

share the space with human, desirable compliance is represented by the solid line in figure 8. It is difficult to realize such characteristics by passive compliance only. In some cases, it needs to design such compliance as example 1 or 2 shown in figure 8. In example 1, the compliance in low frequency is low for the purpose of improvement of the work performance. On the other hand, in example 2, the compliance in the low frequency is high for the safety issue. The curve shaping of compliance in frequency domain is technical demand.

The biggest problem of active compliance is robustness. By the shortage of the actuator power, small resolution and so on, the closed loop system becomes unstable easily if the controller has high gain. To get a robust controller which realizes the desirable compliance is important.

In this paper, we design hybrid compliance of active compliance which is programmable and passive compliance which is stable. Their roles are split into high and low frequency domain. H_∞ control theory is used for the design of controller of the active compliance.

4 H_∞ hybrid compliance

4.1 H_∞ control [8]

Consider the generalized control system as

$$\begin{bmatrix} z \\ y \end{bmatrix} = \begin{bmatrix} G_{11} & G_{12} \\ G_{21} & G_{22} \end{bmatrix} \begin{bmatrix} f \\ u \end{bmatrix} \quad (7)$$

H_∞ controller satisfies the following inequality.

$$\|G_{zf}\|_\infty < 1 \quad (8)$$

$$G_{zf} = G_{11} - G_{12}(I + CG_{21})^{-1}CG_{21} \quad (9)$$

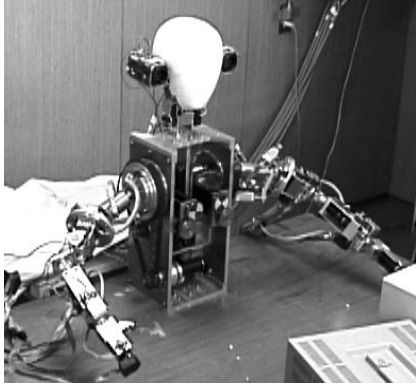


Figure 4: Torso robot

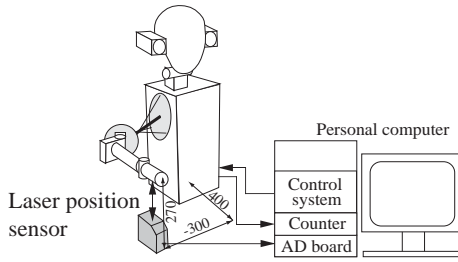


Figure 5: Experimental setup

Here G_{zf} means the transfer function of f to z , and $\|\cdot\|_\infty$ means H_∞ norm which is defined as

$$\|G(s)\|_\infty := \sup_{0 < \omega < \infty} |G(j\omega)| \quad (10)$$

For the controller design of active compliance, we are going to make use of concept of the generalized control system and the weighting function for H_∞ control theory.

4.2 Controller design

4.2.1 Configuration and specifications of the controller

Suppose that the humanoid P is stabilized by the local feedback controller C_ℓ as shown in figure 9. P has divided into the modeled and un-modeled parts whose outputs are θ_m and θ_u respectively. For example, the dynamics of the elastic link is the un-modeled part because it is difficult to observe the strain of this link. θ_u is not available for the local feedback controller C_ℓ . y_0 is the reference signal of the position and orientation of the end effector y . θ_r is the rotation angle of each joints, τ is the torque of actuators and K, I are operators of kinematics and inverse kinematics respectively.

The outer force acting on the end of the hand is represented as shown in figure 10. Here, f is small

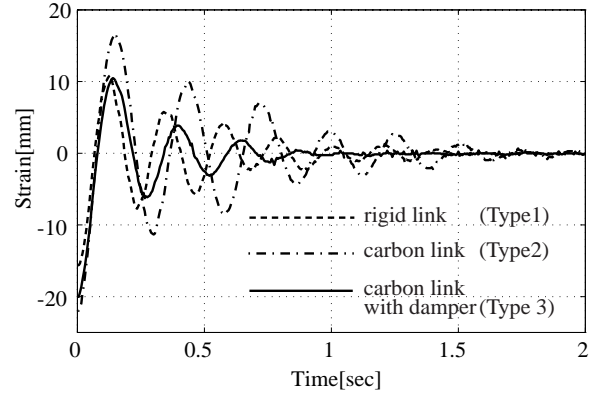


Figure 6: Impulse responses

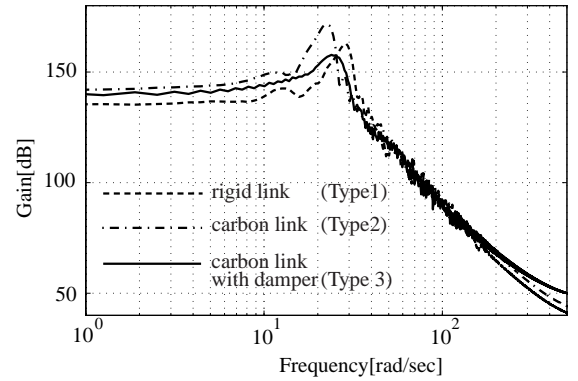


Figure 7: Frequency analysis

enough and J_u, J_m are jacobian defined as follows.

$$\dot{y} = \begin{bmatrix} J_u & J_m \end{bmatrix} \begin{bmatrix} \dot{\theta}_u \\ \dot{\theta}_m \end{bmatrix} \quad (11)$$

P is divided into modeled parts P_{m1}, P_{m2} and un-modeled parts P_{u1}, P_{u2} .

$$\begin{bmatrix} \theta_u \\ \theta_m \end{bmatrix} = P \begin{bmatrix} \tau_u \\ \tau + \tau_m \end{bmatrix} \quad (12)$$

$$P := \begin{bmatrix} P_{u1} & P_{u2} \\ P_{m1} & P_{m2} \end{bmatrix} \quad (13)$$

The transfer function from f to y defined as follows

$$y = G_{yf}^{open} f \quad (14)$$

represents humanoid's dynamic compliance designed by the passive compliance only.

For the vibration control, we design the controller C_v shown in figure 11. The input of C_v is the error of the reference y_0 and y which is observed by visual

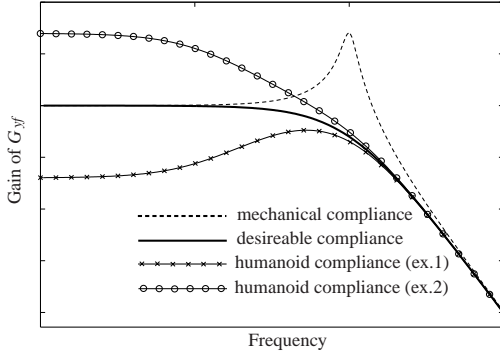


Figure 8: Example of the humanoid compliance

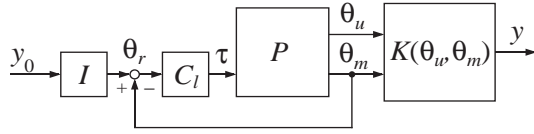


Figure 9: Local feedback system

sensors or velocity sensors. The strain is small enough to assume $y - y_0 \ll 1$. $[\cdot]^\dagger$ means a pseudo inverse. The transfer function from f to y of the closed loop system using controller C_v is defined as follows.

$$y = G_{yf}^{close} f \quad (15)$$

Because the gain characteristic of G_{yf} means active/passive dynamic compliance in frequency domain, we can get desirable humanoid dynamic compliance by shaping its characteristic.

When C_v is equal to zero, Δy

$$\Delta y := y - y_0 \quad (16)$$

is represented as follows.

$$\Delta y = K(\theta_u, \theta_m) G \begin{bmatrix} f \\ y_0 \\ u \end{bmatrix} - y_0 \quad (17)$$

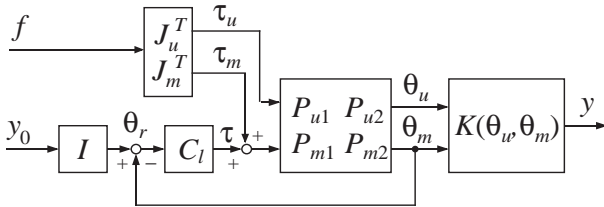


Figure 10: Disturbance input

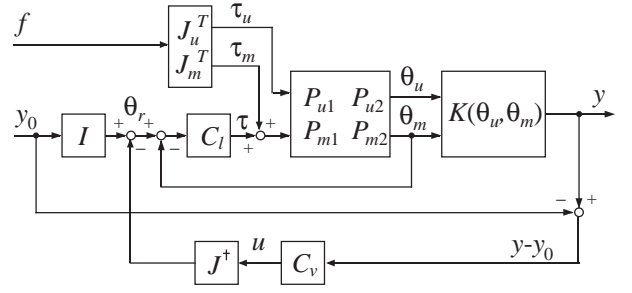


Figure 11: Vibration control system

$$G = \begin{bmatrix} G_s G_m & G_t I & -G_t J_m^\dagger \\ G_u - P_{u2} C_l G_s G_m & P_{u2} C_l G_s I & -P_{u2} C_l G_s J_m^\dagger \end{bmatrix} \quad (18)$$

$$G_s := (E + P_m C_l)^{-1} \quad (19)$$

$$G_t := E - G_s \quad (20)$$

$$G_u := P_{u1} J_u^T + P_{u2} J_m^T \quad (21)$$

$$G_m := P_{m1} J_u^T + P_{m2} J_m^T \quad (22)$$

E : Identity matrix

Because the terms concerned to y_0 in the right hand side of equation (17) is non-affine term depending only on C_l , we can neglect them in the design stage of C_v . The equation (17) is simplified as follows.

$$\Delta y = \begin{bmatrix} \bar{G}_f & \bar{G}_u \end{bmatrix} \begin{bmatrix} f \\ u \end{bmatrix} \quad (23)$$

In the following, the generalized control system for designing C_v is introduced. The purposes of C_v are as follows.

1. The dynamic compliance of the controlled system is shaped by C_v in the frequency domain.
2. In the high frequency domain, C_v does not work for a robust stability.

4.2.2 Generalized control system

Considering the closed loop specifications, the generalized control system is set as shown in figure 12, where W_1 , W_2 and W_3 are the weighting functions. Because H_∞ norm of the transfer function from f to z_1 of the closed loop system is less than 1, the following inequalities are satisfied in almost all frequency.

$$\|G_{yf}^{close} W_1\|_\infty < 1 \quad (24)$$

$$|G_{yf}^{close}| < |W_1^{-1}| \quad (25)$$

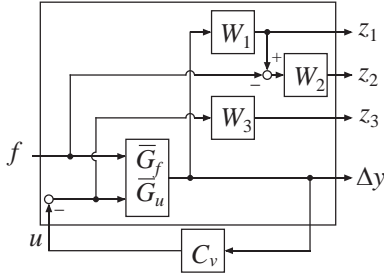


Figure 12: Generalized control system for design of C_v

These mean that W_1 decides the upper bound of the dynamic compliance. And by the satisfaction of the following inequality

$$\|W_2 (E - G_{yf}^{close} W_1)\|_{\infty} < 1 \quad (26)$$

the following is satisfied in any frequency where the gain of W_2 is large enough.

$$W_1^{-1} \simeq G_{yf}^{close} \quad (27)$$

This means that W_2 decides the lower bound of the dynamic compliance. The following inequality

$$\|W_3 (E + C_v \bar{G}_u)^{-1} C_v \bar{G}_f\|_{\infty} < 1 \quad (28)$$

ensures the robust stability of the closed loop system.

By using the H_{∞} controller, we can get the robust controller which satisfies the design specifications, upper and lower bound of the active/passive dynamic compliance.

5 Experimental evaluation

5.1 Configuration of the control object

For simplicity, we focus on one parameter of the position and orientation parameters of the end effector, and the configuration of the torso robot is fixed. The compliance of the local motion is considered. P is a linear system and the jacobian is a fixed number matrix.

5.2 System identification

Because models of \bar{G}_f , \bar{G}_u are needed for the design of H_{∞} controller, we identify their models. The model of \bar{G}_u is identified using M-sequence signal [10] as the Output Error (OE) model \bar{G}_u^m . \bar{G}_f is identified using the experimental result in figure 6 as an ARX model \bar{G}_f^m . The identified models are as follows. They have

a resonate frequency at $\omega = 23.8[\text{rad/s}]$.

$$\bar{G}_u^m = \frac{-1.47 \times 10^{-5} (s + 6975)(s + 34.7)}{(s + 2.76 + 23.8j)(s + 2.76 - 23.8j)} \quad (29)$$

$$\bar{G}_f^m = \frac{5.48 \times 10^{-2} (s + 26.7 + 135j)(s + 26.7 - 135j)}{(s + 2.76 + 23.8j)(s + 2.76 - 23.8j)} \quad (30)$$

5.3 Design of the controller

Case 1 Improvement of the work efficiency (lower compliance) Using \bar{G}_u^m and \bar{G}_f^m in equations (29) and (30), we design a controller based on the generalized control system in figure 12. Here, W_1 , W_2 and W_3 are set as follows.

$$W_1 = \frac{7(s + 15)^3}{(s + 5)^2(s + 1000)} \quad (31)$$

$$W_2 = 0 \quad (32)$$

$$W_3 = \frac{290(s + 10)^3}{(s + 1000)^3} \quad (33)$$

The compliance in the low frequency domain should

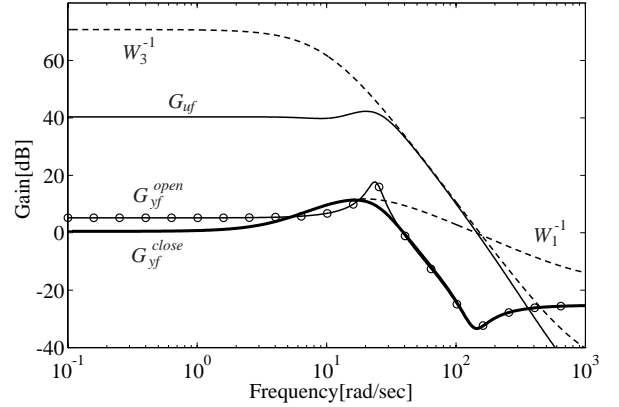


Figure 13: Gain plots (case 1)

be small and the gain at the resonate frequency should be small by the restriction of W_1 .

The gain plots of the designed closed loop system is shown in figure 13. The gain of G_{yf}^{close} is smaller than that of G_{yf}^{open} in low frequency. This means that the strain of the end of the arm caused by the static outer force is small. The controller C_v works effectively in the lower frequency domain. On the other hand, the gains of G_{yf}^{close} and G_{yf}^{open} is same in higher frequency, which means that the controller does not work in high frequency for the robust stability. By using H_{∞} control theory, we can get the controller which satisfies the control configurations in section 4.2.1.

We make the same experiment as figure 5 using the designed controller C_v . The experimental result is shown in figure 14. The dashed line represents the

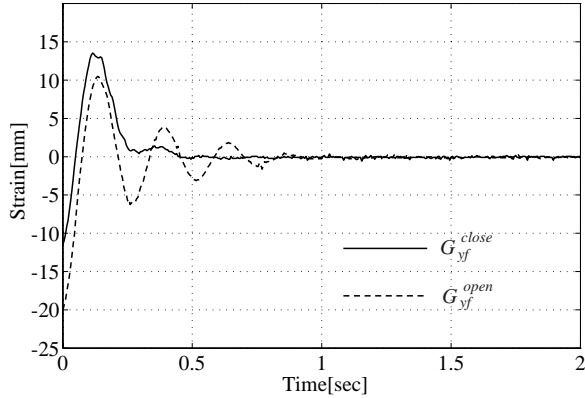


Figure 14: Impulse responses (case 1)

response as of passive compliance using carbon fiber link with a damper in figure 6. The initial conditions of these responses mean that we can get half compliance as much as passive compliance. In general case, it is difficult to get a higher gain controller for the low compliance because of the robust stability. However, because C_v does not work in the high frequency domain, we may not be worried about this problem by using the proposed method.

Case 2 Improvement of the safety (higher compliance) Secondly, we design the controller considering following specifications.

- Get the higher compliance in lower frequency by the active controller, which means

$$|G_{yf}^{open}| < |G_{yf}^{close}| \quad (34)$$

should be satisfied.

- The gain at the resonate frequency should be smaller.

The weighting functions are set as follows.

$$W_1 = \frac{12(s+20)}{s+1000} \quad (35)$$

$$W_2 = \frac{65}{(s+5)^2} \quad (36)$$

$$W_3 = \frac{214(s+10)^3}{(s+1000)^3} \quad (37)$$

Figure 15 shows the gain characteristic of the designed closed loop system. By the restriction of W_2 , G_{yf}^{close}

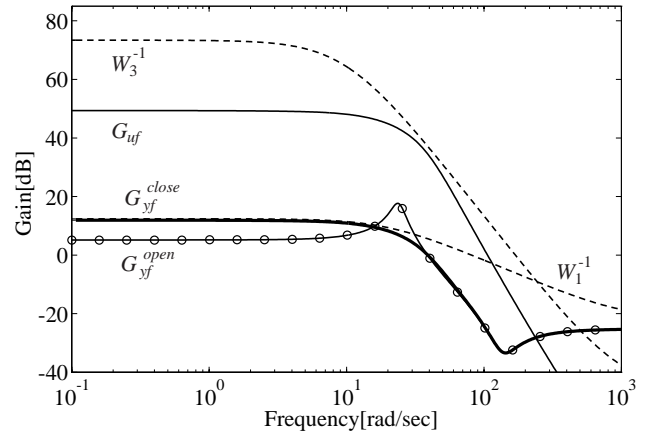


Figure 15: Gain plots (case 2)

is close to W_1^{-1} in lower frequency. Because this gain characteristic is larger than the gain of G_{yf}^{open} , we can get the high active/passive dynamic compliance. The impulse responses with the initial condition are shown in figure 16. This figure shows that we can get the

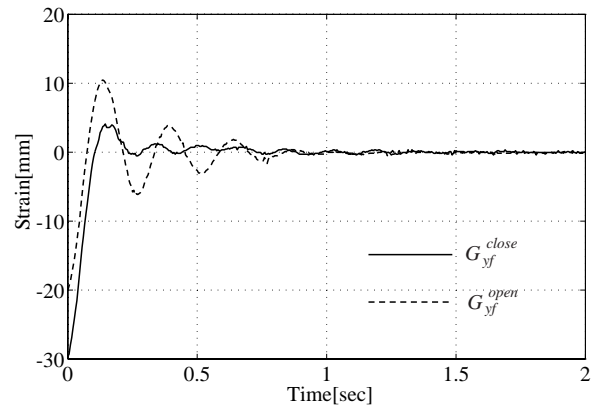


Figure 16: Impulse responses (case 2)

1.5 times active/passive compliance as high as passive compliance.

6 Considerations

By the design and experiments of active/passive compliance, we get the following knowledge.

- To realize extreme higher or lower compliance, it needs much actuator power, which is undesirable from the robust point of view. By setting a pole

in low frequency on W_1 , we can avoid this problem. However in this case, the closed loop system G_{yf}^{close} has a pole in low frequency, which causes slow convergence of the response.

- For the control of the mechanical resonance, it needs a negative feedback, on the other hand, it needs a positive feedback for the realization of the higher active compliance, which means that controller should turn its phase characteristic in one frequency. To realize this characteristic under the restriction of the lower gain of the controller, the controller C_v tends to have unstable poles, which is not desirable from the robust point of view.
- In this section, we discuss on the compliance of one position variable. By measuring all variables of the position and orientation by visual or velocity sensors, we can control the multi direction of compliance. On the cybernetic shoulder, by measuring θ_{41} , θ_{42} and L_3 in figure 2, the position and orientation of the end effector in the absolute coordinate can be calculated.

It is important to design appropriate humanoid compliance considering work, environment and safety, by which the humanoid robot would be able to throw a ball with a small actuator power and to jump higher, which are future works.

7 Conclusions

The results of this paper are as follows.

1. We designed three types of elastic and viscous links for the cybernetic shoulder, which realized an appropriate compliance for humanoid robots.
2. We have discussed the importance of designing compliance for humanoid robots which share the space and environment with the humans.
3. We proposed the compliance design method using H_∞ control theory where the role of active and passive compliance are split into the frequency domain, which is based on that active compliance works well in the lower frequency domain and does not in the high frequency domain.
4. We evaluated the efficiency of the proposed method by experiment using a torso robot with the cybernetic shoulder.

This research was supported by the Research for the Future Program, the Japan Society for the Promotion of Science (Project No. JSPS-RFTF96P00801).

References

- [1] R.P.C.Paul and B.Shimano : Compliance and Control, Proc. of the 1976 Joint Automatic Control Conference, pp.694-699, 1976.
- [2] H.Hanafusa and H.Asada : Stable Pretension by a Robot Hand with Elastic Fingers, Proc. of the 7th International Symposium on Industrial Robots, pp.361-368, 1977.
- [3] N.Hogan : Mechanical Impedance Control in Assistive Devices and Manipulators, Proc. of the 1980 Joint Automatic Control Conference, pp.TA10-B, 1980.
- [4] J.K.Salisbury : Active Stiffness Control of a Manipulator in Cartesian Coordinates, Proc. of the IEEE Conference on Decision and Control, 1980.
- [5] N.Hogan : Impedance Control: An Approach to Manipulation: Part 1~3, ASME Journal of Dynamic Systems, Measurement and Control, Vol.107, pp.1-24, 1985.
- [6] K.F.L-Kovitz, J.E.Colgate and S.D.R.Carnes: Design of Components for Programmable Passive Impedance, Proc. of IEEE International Conference on Robotics and Automation, pp.1476-1481, 1991.
- [7] M.Okada and Y.Nakamura: Development of the Cybernetic Shoulder - A Three DOF Mechanism that Imitates Biological Shoulder-Motion -, Proc. of IEEE/RSJ International Conference on Intelligent Robots and Systems, Vol.2, pp.543-548 (1999)
- [8] K.Glover and J.C.Doyle (H.Nijmeijer, J. M. Schumacher eds.) : A State Space Approach to H_∞ Optimal Control, Three Decades of Mathematical System Theory, Springer-Verlag, pp.179-218, 1994.
- [9] M.E.Rosheim: Robot Evolution, The Development of Anthropotics; JOHN & SONS, INC., (1994)
- [10] L.Ljüing : System Identification - Theory for the User, Prentice-Hall, 1987.